

COMPARATIVE ASSESSMENT OF PLUNGING JET SCOUR DEPTH PREDICTIVE FORMULAE UNDER VARIABLE SOIL MOISTURE CONDITIONS

Nilakshan Balasubramaniam¹, Ravindra Jayaratne², Taeksang Kim³ and Jeremy Bricker⁴

This study investigates the accuracy and reliability of various scour predictive models exposed to tsunami-induced waves, using experimental data obtained from controlled laboratory tests in the wave flume at the University of East London. Varying soil conditions, including dry (oven-dried) and wet (partially saturated) sand were tested to assess the influence of soil moisture on the scour effects. Using the dam-break method to simulate tsunamis, the study examined four different hydraulic conditions to replicate varying tidal scenarios. Scour depths, both maximum and equilibrium values, were recorded using a combination of lidar sensors, high-precision digital point gauges, and slow-motion video cameras. The wave characteristics were then derived from the data collected during the experiments including lidar data and video files. The results were compared against well-established mathematical models from previous studies, such as those by Chee and Yuen (1985), Novak et al. (1990), Fahlbusch et al. (1994), Noguchi et al. (1997), Dehghani et al. (2010), Jayaratne et al. (2016) and Gelfi et al. (2022). The study compares the predicted scour depths from these models against laboratory measured data under both wet and dry soil conditions. Results indicate varying levels of predictive accuracy, with some models performing better under specific conditions. The study reveals how soil moisture significantly impacts scour depth and structural stability during extreme wave events like tsunamis. It emphasises the importance of refining existing predictive models to account for the dynamic interaction between soil properties and hydraulic forces. Recommendations are provided to advance these models by incorporating additional scour dynamics.

Keywords: Plunging jet; equilibrium and maximum scour depths; tsunamis; laboratory experiments

INTRODUCTION

Tsunamis are classified as long waves generally caused by subsea-level disturbances like earthquakes, landslides, volcanic eruptions, meteorites and even explosions. They are some of the most daunting and intricate natural disasters known to humans, which can impact almost every coastal area around the world. These waves can travel thousands of kilometres from their origin, and thereby have the potential to cause destruction far from their point of origin (St-Germain, Nistor and Townsend, 2012). Over the last 20 years, numerous tsunamis occurred around the globe of which the 2004 Indian Ocean tsunami and the 2011 Great East Japan earthquake and tsunami resulted in extensive damage both to lives and structures. The 2004 tsunami resulted in more than 220,000 casualties and the 2011 tsunami resulted in around 19,100 casualties. The 2011 tsunami event also led to an estimated damage exceeding US\$ 319 billion (St-Germain *et al.*, 2014).

Seawalls are a very important line of defence in coastal environments. They are built along the coastline to prevent damage in nearshore regions. They can be designed and constructed using a variety of materials to meet specific local needs, making them a versatile option for many communities. However, vertical seawalls are relatively ineffective in dissipating wave energy. Thus, the impact of waves on these structures results in increased scouring at the base of the seawall, which is a major factor contributing to their failure (Kraus *et al.*, 1996). Since seawalls serve as the first line of defence against coastal erosion and are widely installed worldwide, their tendency to fail prematurely under extreme wave conditions underscores the importance of investigating their stability under various extreme wave conditions.

There is very limited number of field data available about tsunami-induced scour around coastal structures. Although we have experienced two major tsunami events in this century namely the 2004 Indian Ocean tsunami and the 2011 Great East Japan earthquake and tsunami, not a significant amount of tsunami-induced scour field data is available due to the 2004 tsunami. Few researchers have analysed tsunami-induced scour data after the 2011 Tohoku tsunami including Bricker et al. (2012), who investigated scour around coastal defence structures, specially focussing on seawalls, Jayaratne et al. (2014) who investigated about scour around coastal dikes, Tonkin et al. (2014) about the scour around buildings and roads and Wilson et al. (2012) around harbours.

A significant drawback with the findings of these results is that they often tend to focus the post-tsunami scour depths and extent. The values recorded by post-tsunami research teams may differ significantly from those values during a tsunami. The scour characteristics measured by the post-disaster

^{1,2}Department of Engineering & Construction, School of Architecture, Computing and Engineering, University of East London, Docklands Campus, 4-6 University Way, London E16 2RD, UK.

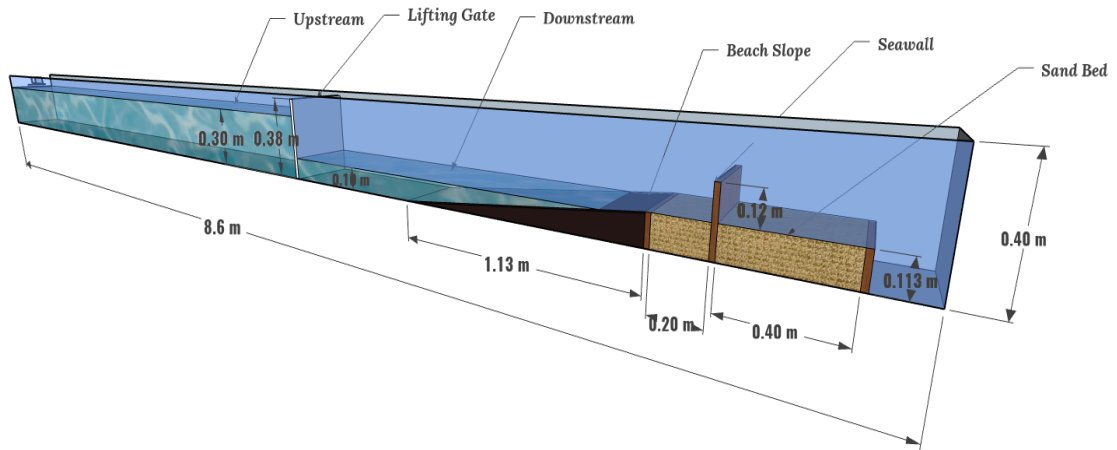
^{3,4}Department of Civil and Environmental Engineering, University of Michigan, 2350 Hayward St, Ann Arbor, MI 48109, USA.

survey teams represent the equilibrium scour depth, which is the value after the event has finished. However, during the tsunami event, the force of the impinging jet can create a deeper scour hole (maximum scour) than what is eventually measured by the survey teams after the tsunami event is over. As the impinging jet weakens and eventually stops, the soil particles that were set in motion may still be within the region of the scour hole and settle back into the scour hole. This results in a measured scour depth value is less than the maximum scour depth that occurs during the tsunami event (Jayaratne *et al.*, 2023). Thus, a robust model which can predict both the maximum and equilibrium scour depths is of paramount importance.

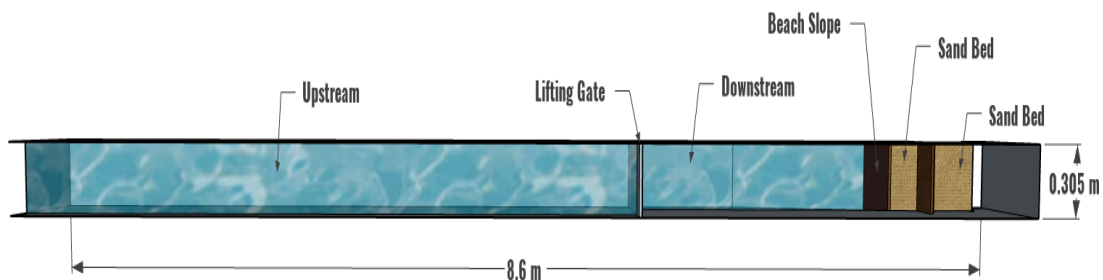
The primary aim of this study is to evaluate the accuracy of the existing scour depth predictive models developed by various researchers by analysing the predictions derived from their models with experimental data acquired at the University of East London. Furthermore, this study will analyse the correlation between model predictions and the observed maximum and equilibrium scour depths under both wet and dry soil conditions. For this analysis, the study uses scour predictive models that can determine the scour behind a vertical seawall as the result of a plunging jet. Finally, this research will identify the most reliable mathematical models and highlight potential areas of improvement for better accuracy.

MATERIALS AND METHODS

Fully controlled laboratory experiments were carried out in the wave flume at the hydraulic engineering laboratory of the University of East London. The wave flume (Fig. 1) measured 8.6 m in length, with a width of 0.315 m and a depth of 0.305 m. A model seawall made of concrete with a height of 12 cm above the sand level was installed in the flume with a prototype scale ratio of 1:25. The seawall was installed in the flume inside sandboxes such that the length of the seaward sandbox was 20 cm and landward sand box was 40 cm. The seawall was fixed to the flume, ensuring that there would be no wall movement during the wave impact, uprush and overflowing.



(a) Experimental set-up in the wave flume at University of East London.



(b) Plan view of the wave flume at University of East London.

Figure 1. Schematic sketch of wave flume at the University of East London.

Solitary tsunami waves were generated using a lifting gate mechanism. A lifting gate made of Perspex was used to store water in the upstream section of the flume, maintaining a constant upstream water depth (H_u) of 30 cm for all experimental runs. During the experiments, the lifting gate was rapidly lifted to generate a solitary wave. Water depth just after the lifting gate, referred to as downstream depth (H_d), varied as an independent variable during the experiments. Four different downstream depths (2.5, 5, 7.5, 10 cm) were employed.

An impermeable 1:10 slope, made of Perspex with a horizontal length of 113 cm, was placed between the downstream water volume and the sandbox. Sandbox of $20 \times 11.3 \times 30$ cm ($L \times H \times W$) was installed on the seaward side of the seawall whereas sandbox of $40 \times 11.3 \times 30$ cm ($L \times H \times W$) was installed on the landward side. The sandboxes were filled with sand with an average grain diameter of 0.5-1.0 mm. Two soil moisture conditions were used for the experiments: the first was wet soil, and the second was dry soil, where the sand was oven-dried for 24 hours at 1100°C . To ensure accuracy and mitigate errors, experimental runs were repeated three times for each tested hydraulic condition and each soil moisture condition. Table 1 presents the details of the laboratory experiments, outlining the various hydraulic and soil moisture conditions, thereby providing a comprehensive overview of the experimental regime.

Seawall type	Upstream height, H_u (cm)	Downstream height, H_d (cm)	Fill material	Soil condition	Number of tests
Fixed foundation	30.0	2.5	Sand	Wet	3
				Dry	3
		5		Wet	3
				Dry	3
		7.5		Wet	3
				Dry	3
		10		Wet	3
				Dry	3
Total tests					24

The entire duration of the experimental runs, from the generation of solitary wave using a lifting gate to the formation of scour profile by the plunging jet, was captured using multiple high-precision video cameras. Maximum and equilibrium scour depths were measured using a slow-motion video camera and a lidar sensor respectively. Additionally, a high-precision digital point gauge was employed to measure and validate the equilibrium scour depths. After the experiment, video recordings and collected data were analysed to extract maximum and equilibrium scour depths, the extent of the scour hole, wave celerity, overtopping flow height, impingement angle and the tailwater depth (Fig. 2). These parameters were subsequently utilised as inputs to various scour predictive models.

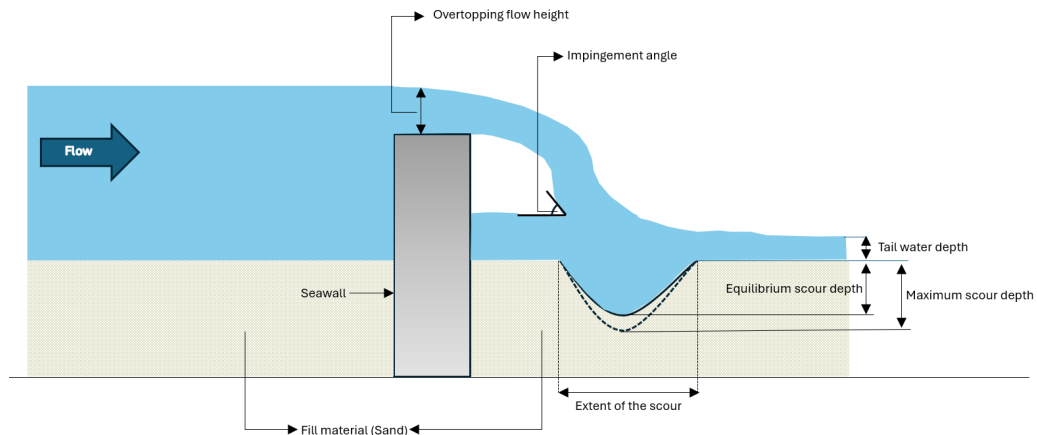


Figure 2. Tsunami wave overtopping a seawall and related parameters.

PREDICTIVE MODELS

Scour is a complex mechanism as the process involves several sediment and hydrodynamic-related parameters. Researchers have experimented and proposed several mathematical models to predict the representative scour depth and extent developed by an overtopping plunging jet.

Stein et al. (1993) discussed the model proposed by Chee and Yuen. (1985) to predict the equilibrium scour depth D_e (m) measured from the original unscoured bed as given in Eq. (1).

$$D_e = J_e \sin \mathcal{X} - h_t \quad (1)$$

where J_e is the length of the jet from its centreline to the point where it enters the tailwater (m), h_t is the depth of the tailwater above the original unscoured bed (m), and \mathcal{X} is the angle of jet impingement ($^\circ$).

Noguchi et al. (1997) as described in Bricker et al. (2012) proposed a predictive formula for scour depth at equilibrium condition. They found that the width R of the eddy created in the scour hole at the toe of the bulkhead under the equilibrium condition (m) can be described by Eq. (2).

$$R = g^{-1/4} q^{1/2} h^{1/4} \quad (2)$$

where g is the gravitational acceleration (ms^{-2}), q is the flow rate per unit length of the bulkhead (m^2s^{-1}), and h is the height of the bulkhead crest above the undisturbed ground level (m). Equilibrium scour depth (m) ε was determined to be $\varepsilon=2.1R$.

Dehghani et al. (2010) employed dimensional analysis to relate the scour depth ε to flow conditions, structural dimensions and upstream Froude number, F_{up} . The equation for the upstream Froude number is given by Eq. (3).

$$F_{up} = \frac{U}{\sqrt{gH}} \quad (3)$$

where U is the average flow speed of the river (ms^{-1}), g is the gravitational acceleration (ms^{-2}), and H is the flow depth (m). Using values computed for F_{up} and using the height of the weir crest h , the surcharge height of water above the weir crest h_1 , the scour depth values ε were computed using information in Table 2.

Table 2. Scour depth values from Dehghani et al. (2010) model as given in Bricker et al. (2012).		
F_{up}	h_1/h	ε/H
$0.058 < F_{up} < 0.076$	0.25	0.7
$0.058 < F_{up} < 0.076$	0.4	1
$0.078 < F_{up} < 0.093$	0.35	0.7
$0.078 < F_{up} < 0.093$	0.45	0.8
$0.096 < F_{up} < 0.137$	0.5	0.7
$0.096 < F_{up} < 0.137$	0.8	1

One drawback with this predictive model is the range of Froude numbers (Fr) they proposed from the experiments. For this study, when Fr exceeded the specified range, the upper boundary of the Fr value was utilised.

Novak et al. (1990) as discussed in Conesa-García and García-Lorenzo (2009) proposed the local scour depth $Y_{m,e}$ is given by Eq. (4).

$$Y_{m,e} = 0.55 \left(6H^{0.25} q^{0.5} \left(\frac{y_0}{D_{90}} \right)^{1/3} - y \right) \quad (4)$$

where H is the step between the upstream energy gradient line and the downstream (landward of structure) water surface (m), q is the unit discharge per unit width (m^2s^{-1}), y is the flow depth in the landward side of the weir (m), y_0 is the initial depth of the water before the scour begins (m) and D_{90} is the particle size corresponding to the 90th percentile of the sample in mm.

Jayaratne et al. (2014) proposed a mathematical formula to predict the representative scour depth on the landward side of a coastal dike based on the field datasets of 2011 Tohoku post-tsunami surveys. Their formula was based on the Buckingham π theorem and measurable field parameters to predict the scour depth. This predictive model has been further enhanced by comparing with laboratory scour depth experiments (Jayaratne et al., 2016) to improve its predictive capability. Their final model is given in Eq. (5).

$$\frac{D_s}{H_{d2}} = \lambda \left(\exp - \left(\frac{\sqrt{H_{d2}}}{2\lambda\sqrt{h} \sin\theta_2} \right)^4 \right) \left\{ \begin{array}{l} h > 0 \\ 10^{-4} < k < 10^{-3} \end{array} \right. \quad (5)$$

where D_s is the depth of scour (m), H_{d2} is the height of coastal dike measured from the leeward toe (m), h is the inundation depth (m), θ_2 is the angle of the leeward slope (radian) and λ is the dimensionless scour coefficient ($=0.85$).

Tonkin et al. (2014) used the model proposed by Fahlbusch et al. (1994) to predict the scour depth d_s as given in Eq. (6).

$$d_s = c_{2v} \sqrt{qU \sin \theta / g} \quad (6)$$

where C_{2v} is the scour coefficient (-), which is equal to 2.8 according to the average value derived from Fahlbusch's et al. (1994) datasets, q represents the discharge per unit width over the overtopped structure (m^2s^{-1}), U denotes the velocity of the jet as it approaches the scour hole (ms^{-1}), θ is the angle ($^\circ$) between the jet at the scour hole and the horizontal plane, and g is the gravitational acceleration (ms^{-2}).

Gelfi et al. (2022) enhanced the model of Jayaratne et al. (2016) by incorporating the effect of median sediment size (D_{50}) on the scour depth. Their model revised the fitted coefficient (λ) to be a function of the median sediment size (D_{50}) to better capture the influence of sediment size on the scour depth. The revised fitted coefficient (λ) will be given by,

$$\lambda_s = 0.89 - 0.44 \times \exp\left(\frac{H_d}{49.74 \times D_{50}}\right) \quad (7)$$

where H_d is the height (m) of the coastal structure measured from the leeward toe. The updated predictive formula is given in Eq. (8),

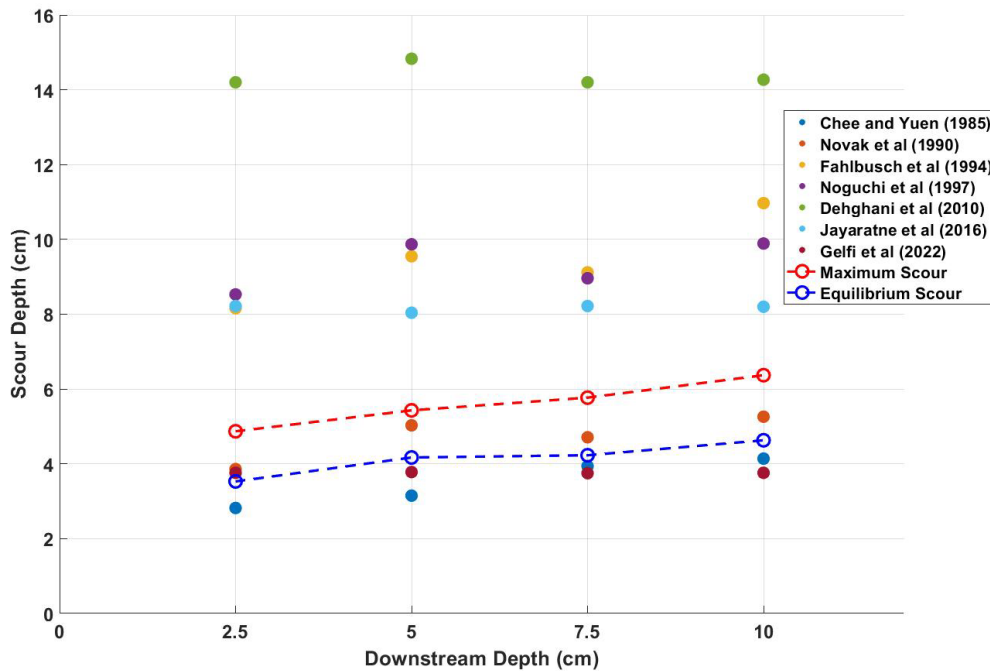
$$\frac{D_s}{H_d} = \lambda_s \times \exp\left(-\frac{\sqrt{H_d}}{2.5\sqrt{h} \sin \theta}\right) \quad (8)$$

where θ is the angle ($^\circ$) of the leeward slope and D_s is the scour depth (m).

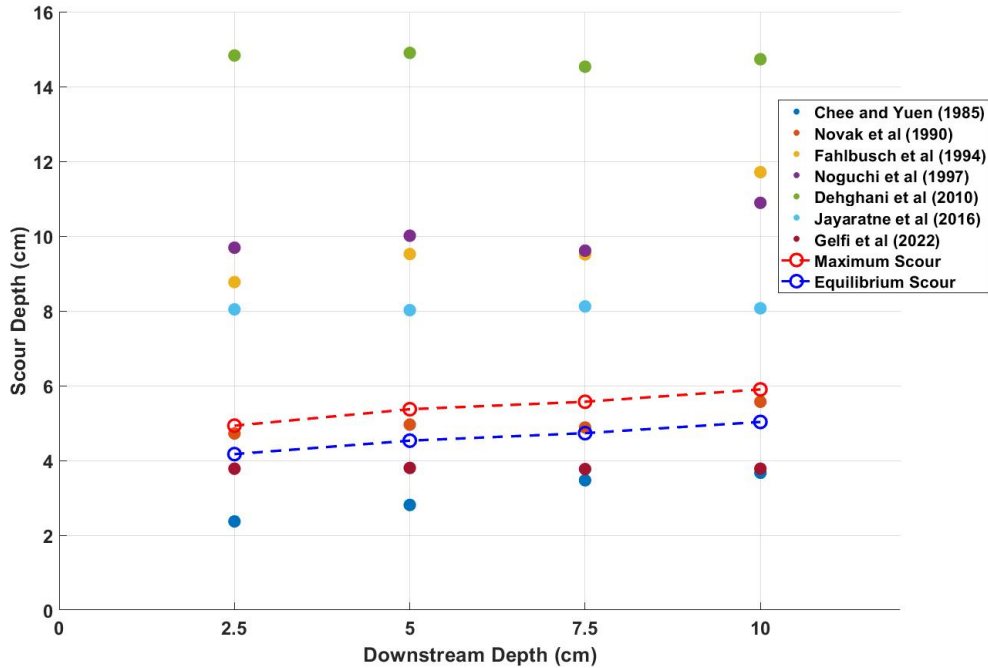
Hydrodynamic, sediment and scour depth values obtained from the laboratory experiments were used in the scour depth predictive equations [Eq. (1) - Eq. (8)] mentioned above. The predictive scour depths from above mathematical models were then compared with experimental maximum and equilibrium depths obtained during the laboratory tests at University of East London.

RESULTS

Figure 3 presents the scour depths averaged over repeated tests, including the maximum and equilibrium depths, along with the values predicted by scour predictive models for both partially saturated (wet) and dry (oven dried) soil moisture conditions for varying hydraulic conditions.



(a) Predicted and measured scour depth D_s (cm) in partially saturated (wet) soil moisture conditions.



(b) Predicted and measured scour depth D_s (cm) in dry (oven dried) soil moisture conditions

Figure 3. Scour depths on a 12 cm cantilever seawall with overtopping discharges (0.0126-0.0189 m³/s) comparing with wet and dry soil conditions for varying downstream depths.

It can be observed that, in both wet and dry soil moisture conditions, the scour depth generally increases as the downstream water depth changes from 2.5 to 10 cm. The scour depth trend is observed to be linear, indicating that larger downstream depths may result in more significant scouring due to increased flow velocity and water volume impacting the seawall. The wet soil condition consistently shows higher scour depths compared to the dry condition for tested downstream depths. This suggests that the soil moisture content plays a significant role in the scour process. This may be caused due to the reduced soil effective stress and increased susceptibility to erosion in wet conditions. In wet soil conditions, the presence of water increases pore pressure. This will result in lowering the critical shear stress needed for sediment mobilisation. According to the Shields parameter, sediment is more easily eroded when the flow-induced shear stress exceeds the critical shear stress. Wet soils are thus more susceptible to erosion under the same flow conditions, leading to greater scour depths compared to dry soils.

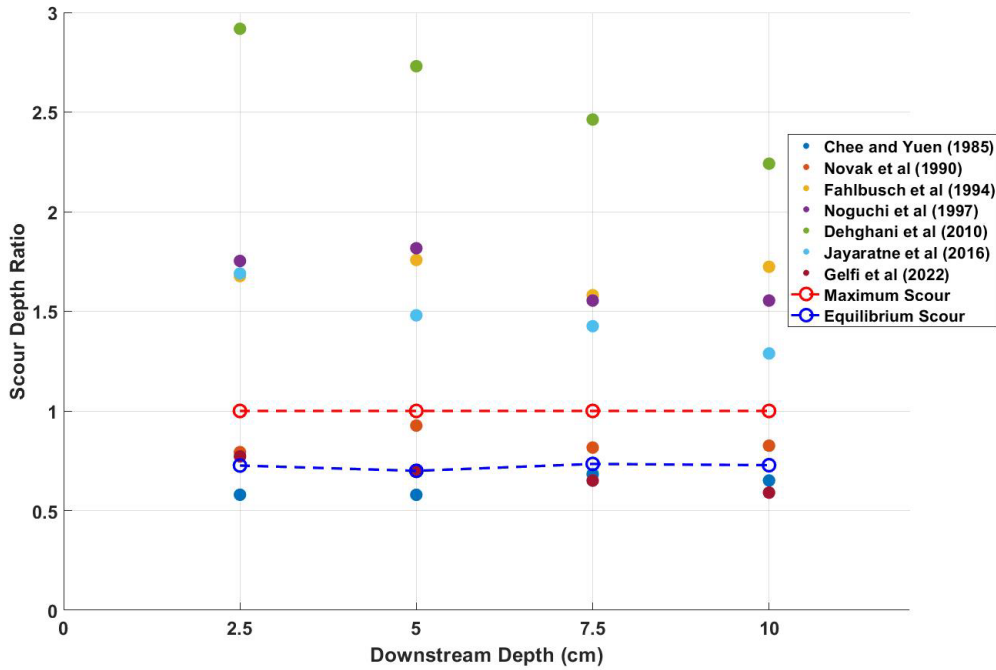
Chee and Yuen (1985), Novak et al. (1990), Jayaratne et al. (2016) and Gelfi et al. (2022) accurately predict equilibrium scour depths, especially in wet conditions. However, discrepancies exist in some models (e.g. Noguchi et al (1987); Dehghani et al. (2010)), particularly at higher downstream depths and when soil moisture condition changes. This suggests that the variations in soil characteristics such as moisture content level and/or wave parameters based on which these models were developed could influence results.

Both Figures 3(a) and 3(b) show clear differences between maximum and equilibrium scour depths. The maximum scour depth is consistently higher than the equilibrium scour depths for all tested downstream depths. This distinctive difference is crucial as it highlights the impact of the wave can be more severe than it seems and may eventually cause the failure of the structure. However, the scour depth eventually stabilises to a lower equilibrium value because of the settlement of soil particles as the flow weakens. This pattern is consistent in both wet and dry soil conditions, emphasising the dynamic nature of scour process where initial turbulence gradually diminishes, and the particles settle back into the scour hole as the flow weakens.

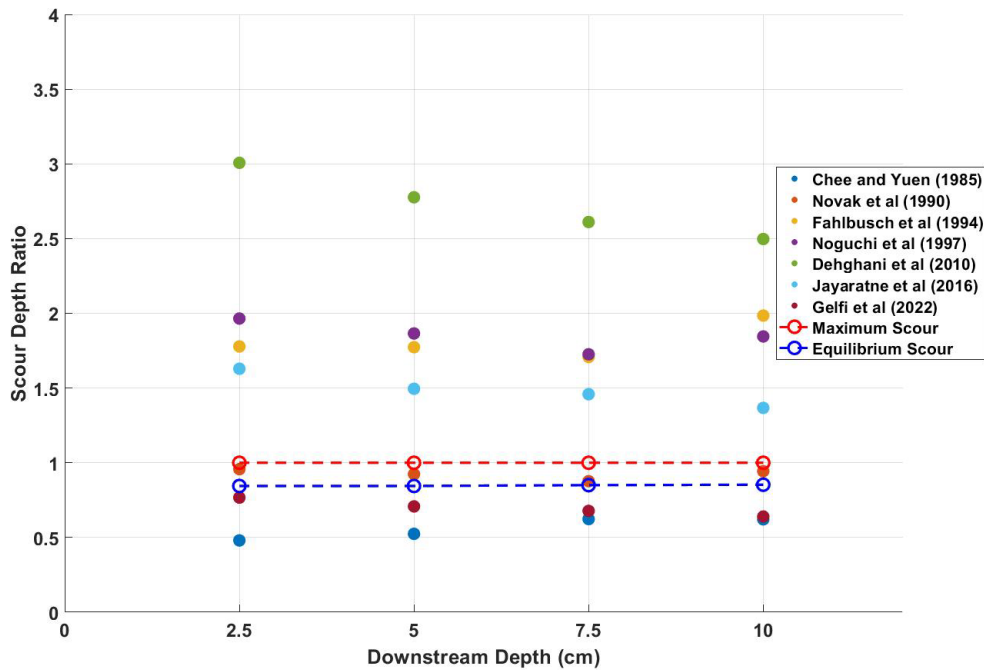
Figure 4 depicts the normalised maximum and equilibrium scour depths obtained under both wet and dry soil conditions for the scour predictive models used in this study. The normalised scour depth is defined by Eq. (9).

$$D_{\text{norm}} = \frac{D_{\text{s(model)}}}{D_{\text{s(experiment)}}} \quad (9)$$

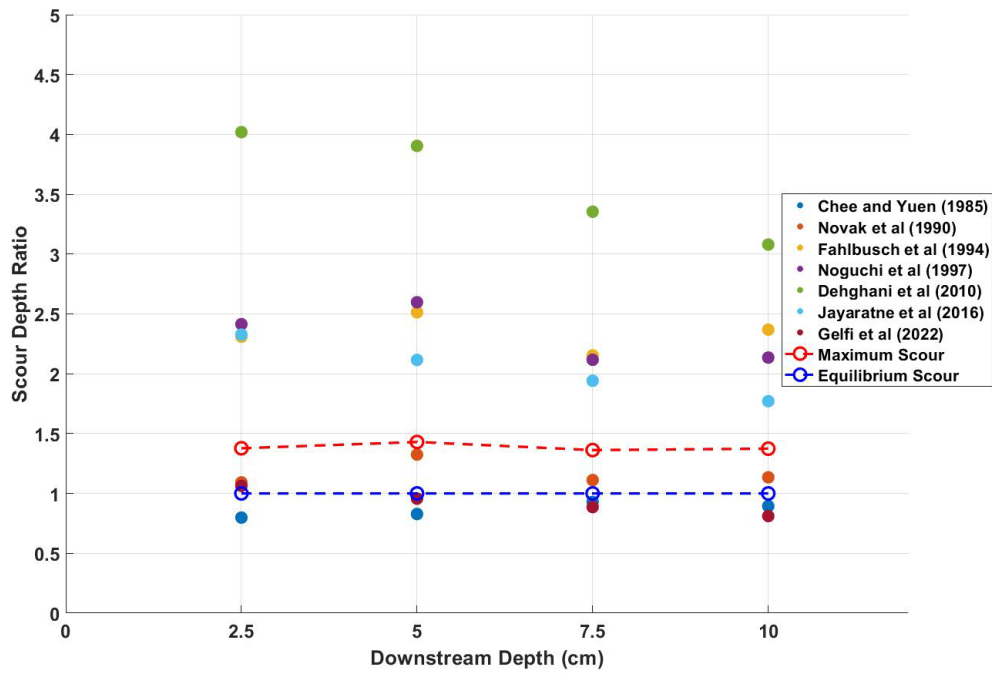
where D_{norm} is the dimensionless normalised scour depth. $D_{\text{s(model)}}$ is the scour depth predicted by mathematical models and $D_{\text{s(experiment)}}$ is the scour depth (maximum or equilibrium) measured in the laboratory experiments.



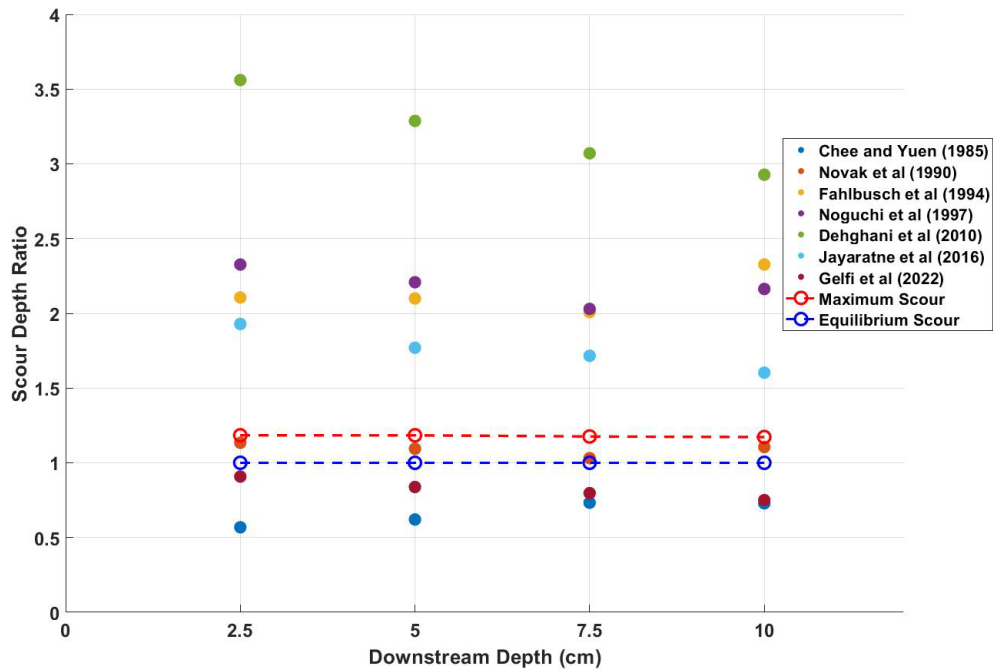
(a) Scour depth normalised by maximum scour depth ($D_s/D_{s,\text{MAX}}$) for wet soil.



(b) Scour depth normalised by maximum scour depth ($D_s/D_{s,\text{MAX}}$) for dry soil.



(c) Scour depth normalised by equilibrium scour depth ($D_s/D_{s,EQM}$) for wet soil.



(d) Scour depth normalised by equilibrium scour depth ($D_s/D_{s,EQM}$) for dry soil.

Figure 4. Comparative analysis of normalised scour depths under wet and dry conditions, using maximum and equilibrium depths as baselines in predictive models.

To analyse how closely each model predicts the equilibrium and maximum scour depths for wet and dry soil moisture conditions, the proximity of normalised scour depth values to unity (1.0) was analysed. Values closer to 1.0 indicate that the predicted scour depth closely matches the measured scour depth (either maximum or equilibrium), which the authors use as a baseline for normalisation.

Normalised to maximum scour depth

Wet condition: Figure 4(a) suggest that models such as Novak et al. (1990), Jayaratne et al. (2016) and Gelfi et al. (2022) consistently estimate closer to the maximum depth for tested hydraulic conditions. However, Novak et al. (1990) and Gelfi et al. (2022) consistently underestimated whereas Jayaratne et al. (2016) overestimated scour depths. Although no significant variations were observed in the results of Chee and Yuen. (1985) and Novak et al. (1990) with varying downstream depths, they underestimated the scour depths.

Dry condition (Fig. 4(b)): Novak et al. (1990) and Gelfi et al. (2022) predicted scour depths close to the measured values. Although consistency was observed in the predicted depths by Fahlbusch et al. (1994) and Jayaratne et al. (2016) they overestimated the scour values.

Overall, it was observed that Novak et al. (1990), Jayaratne et al. (2016) and Gelfi et al. (2022) did not vary much with the varying soil moisture conditions (normalised values from 0.8-0.95 and 1.3-1.7), although these methods under-estimated and over-estimated the scour values respectively. On the contrary, the normalised value of Dehghani et al. (2010) with maximum depth ranged from 2.2-3.0.

Normalised to equilibrium scour depth

Wet condition (Fig. 4(c)): Generally, there is deviation between model predictive values of normalised equilibrium depth compared to the normalised maximum depths. Models presented by Chee and Yuen. (1985), Novak et al. (1990) and Gelfi et al. (2022) estimated depth close to the equilibrium depth with some under- and over-prediction.

Dry condition (Fig. 4(b)): Similar to the maximum depth, the values under this soil moisture condition tend to be less scattered. Model results of Novak et al. (1990) and Gelfi et al. (2022) appear to predict closer to the equilibrium depths while results of Dehghani et al. (2010) seem to be much over-estimated.

Overall, the Novak et al. (1990) and Gelfi et al. (2022) predicts the equilibrium scour depth close to the experimental values in both wet and dry soil conditions. While Noguchi et al. (1997) and Jayaratne et al. (2016) show consistency across both soil moisture conditions, however both models over-estimated the equilibrium depth.

DISCUSSION

It was observed that the tested mathematical models tend to better predict scour in dry soil conditions than in wet conditions. This is likely due to those models having themselves been formulated empirically using dry soil conditions. The model proposed by Novak et al. (1990) and Gelfi et al. (2022) are more robust in predicting maximum and equilibrium depths regardless of the soil moisture condition. Models including Noguchi et al. (1997) and Jayaratne et al. (2016) exhibited consistent predictive depths for both wet and dry conditions, however their models over-estimated equilibrium depth and often were close to maximum scour depth. The difference in performance between wet and dry conditions suggests that models should be carefully calibrated based on the soil moisture content, which significantly affects scour dynamics around the coastal structure.

To understand why the predictions by various mathematical models varied in the analysis of scour caused by plunging jet, it is essential to consider several factors. This includes model characteristics such as the parameters considered, the experimental setup, and the analytical methods employed by the researchers for model development.

Jayaratne et al. (2016) focused on tsunami waves overflowing coastal structures, using a series of laboratory experiments to simulate tsunami-induced scour at several coastal dike geometries. This study considered complex interactions such as wave celerity, wave overflowing and wave pressure.

Dehghani et al. (2010) studied the scour in the landward side of overran overflowed weir. They studied the compound effect of flow velocity and directionality, which may affect the scour dynamics. This flow model can create variable flow dynamics at the base of the structure, leading to divergent scour patterns. However, the wave dynamics in the current study were different than that of Dehghani et al. (2010).

Chee and Yuen (1985) investigated erosion in unconsolidated gravel beds, focusing on sediment transport dynamics under steady flow conditions. The physical properties of gravel such as size and consolidation, play a critical role in how it responds to scouring forces, potentially resulting in different scour depths compared to finer sediment which were used in this study.

Noguchi et al. (1997) emphasised the role of turbulence and vortices at the plunging point, which significantly influences the scour depth. The intensity and interaction of these vortices with the seabed can lead to deeper or more widespread scour depending on the experimental conditions. Fahlbusch et al.

(1994) considered the duration of exposure and the cyclic nature of the waves in their analysis. They discussed how these can affect soil consolidation and respond to repeated forcing.

Most of the methods considered did not consider the consolidation of soil as a factor which can affect plunging jet scour. Soil moisture and consolidation, as explored by Chee and Yuen (1985), significantly affect the scour resistance of the material. Wet unconsolidated sand has more chance of being washed away than dry consolidated sand.

These differences in scour prediction by various mathematical models underscores the importance of selecting the appropriate model. The selected model should closely align with the specific physical conditions and expected flow characteristics of the coastal defence structure selected. Understanding these differences in-depth can help in refining the predictive accuracy of scour depth models and tailoring them to specific coastal engineering structure design.

ACKNOWLEDGMENTS

The authors like to extend their sincere gratitude to the Royal Society, UK for its financial support, for the laboratory experiments conducted at the University of East London, described in this study.

REFERENCES

- Bricker, J.D., Francis, M. and Nakayama, A. 2012. Scour depths near coastal structures due to the 2011 Tohoku Tsunami, *Journal of Hydraulic Research*, 50(6), 637–641. Available at: <https://doi.org/10.1080/00221686.2012.721015>.
- Chee, S.P. and Yuen, E.M. 1985. Erosion of unconsolidated gravel beds, *Journal of Civil Engineering*, 12, 559–566. Available at: www.nrcresearchpress.com.
- Conesa-García, C. and García-Lorenzo, R. 2009. Local scour estimation at check dams in torrential streams in southeast Spain, *Geografiska Annaler, Series A: Physical Geography*, 91(3), 159–177. Available at: <https://doi.org/10.1111/j.1468-0459.2009.00361.x>.
- Dehghani, A.A., Bashiri, H. and Dehghani, N. 2010. Downstream scour of combined flow over weirs and below gates, *Proceedings of the International Conference on Fluvial Hydraulics*. Bundesanstalt für Wasserbau, 1201–1205.
- Fahlbusch, F.E. 1994. Scour in rock riverbeds downstream of large dams. *International Journal on Hydropower & Dams*, Vol. 1, No. 4, 1994, pp. 30-32.
- Gelfi, M., Suzuki, T. and Jayaratne, R. 2022. Sediment size effect on the landward coastal structure scour prediction due to tsunami, *Journal of Japan Society of Civil Engineers*, 78(2), 469–474. Available at: https://doi.org/10.2208/kaigan.78.2_I_469.
- Jayaratne, R., Premaratne, B., Adewale, A., Mikami, T., Matuba, S., Shibayama, T., Esteban, M., Nistor, I. 2016. Failure mechanisms and local scour at coastal structures induced by Tsunami, *Coastal Engineering Journal*. World Scientific. Available at: <https://doi.org/10.1142/S0578563416400179>.
- Jayaratne, R., Abimbola, A., Mikami, T., Matsuba, S., Esteban, M., Shibayama, T. 2014. Predictive model for scour depth of coastal structure failures due to tsunamis, in *Coastal Engineering Proceedings*. Available at: <https://doi.org/10.9753/icce.v34.structures.56>.
- Jayaratne, R., Balasubramaniam, N., Kim, T., Bricker, J. 2023. Failure of seawalls due to tsunami-induced scour, *Coastal Engineering Proceedings*, 37, structures. 72. Available at: <https://doi.org/10.9753/icce.v37.structures.72>.
- Kraus, N., McDougal, W. 1996. The effects of seawalls on the beach: Part I, An updated literature review, *Journal of Coastal Research*, 12(3), 691–701.
- Noguchi, K., Sato, S. and Tanaka, S. 1997. Large-scale model experiment of wave overtopping and frontal surface scouring of revetment due to tsunami run-up, *Annual J. Coastal Engineering* 44.
- Stein, O.R., Julien, P.Y. and Alonso, C. V. 1993. Mechanics of jet scour downstream of a headcut, *Journal of Hydraulic Research*, 31(6), 723–738. Available at: <https://doi.org/10.1080/00221689309498814>.
- St-Germain, P., Nistor, I. and Townsend, R., Shibayama, T. 2014. Smoothed-particle hydrodynamics numerical modeling of structures impacted by tsunami bores', *Journal of Waterway, Port, Coastal, and Ocean Engineering*, 140(1), 66–81. Available at: [https://doi.org/10.1061/\(asce\)ww.1943-5460.0000225](https://doi.org/10.1061/(asce)ww.1943-5460.0000225).
- St-Germain, P., Nistor, I. and Townsend, R. 2012. Numerical modeling of the impact with structures of tsunami bores propagating on dry and wet beds using the SPH method, *International Journal of Protective Structures*, 3(2), 221–255.

- Tonkin, S.P., Francis, M. and Bricker, J.D. 2014. Limits on coastal scour depths due to tsunami, in *International Efforts in Lifeline Earthquake Engineering - Proceedings of the 6th China-Japan-US Trilateral Symposium on Lifeline Earthquake Engineering*. American Society of Civil Engineers (ASCE), 671–678. Available at: <https://doi.org/10.1061/9780784413234.086>.
- Wilson, R., Davenport, C. and Jaffe, B. 2012. Sediment scour and deposition within harbors in California (USA), caused by the March 11, 2011 Tohoku tsunami, *Sedimentary Geology*, 282, 228–240. Available at: <https://doi.org/10.1016/j.sedgeo.2012.06.001>.